*Journal of the Korean Society of Groundwater Environment, Vol. 6, No. 1, pp. 23~32, March, 1999*

# Use of a Solution-Adaptive Grid (SAG) Method for the Solution of the Unsaturated Flow Equation

# 불포화 유동 방정식의 해를 위한 해적응격자법의 이용 연구

Min-Ho Koo(구민호)

**Abstract :** A new numerical method using solution-adaptive grids (SAG) is developed to solve the Richards' equation (RE) for unsaturated flow in porous media. Using a grid generation technique, the SAG method automatically redistributes a fixed number of grid points during the flow process, so that more grid points are clustered in regions of large solution gradients. The method uses the coordinate transformation technique to employ a new transformed RE, which is solved with the standard finite difference method. The movement of grid points is incorporated into the transformed RE, and therefore all computation is performed on fixed grid points of the transformed domain without using any interpolation techniques. Thus, numerical difficulties arising from the movement of the wetting front during the infiltration process have been substantially overcome by the new method. Numerical experiments for an one-dimensional infiltration problem are presented to compare the SAG method to the modified Picard method using a fixed grid. Results show that accuracy of a SAG solution using 41 nodes is comparable with the solution of the fixed grid method using 201 nodes, while it requires only 50% of the CPU time. The global mass balance and the convergence of SAG solutions are strongly affected by the time step size ($\Delta t$) and the weighting parameter ($\gamma$) used for generating solution-adaptive grids. Thus, the method requires automated readjustment of $\Delta t$ and $\gamma$ to yield mass-conservative and convergent solutions, although it may increase computational costs. The method can be effective especially for simulating unsaturated flow and other transport problems involving the propagation of a sharp-front.

**요 약 :** Richards 방정식(RE)의 해를 구하는 새로운 수치해석적인 방법으로 해적응격자(SAG)법을 개발하였다. SAG법은 격자생성법을 이용하여 해의 구배가 큰 영역에 더 많은 수의 격자가 밀집되도록 일정한 수의 격자를 자동으로 재분배한다. 이 방법은 좌표변환기법을 이용하여 지배방정식인 RE를 새로운 좌표에서의 RE로 변환하고 유한차분법을 적용하여 방정식의 해를 구한다. 이때 격자점들의 이동은 변환된 RE에 수식으로 반영되기 때문에 고정된 격자점을 갖는 변환된 영역에서는 해를 구하는 과정에서 내삽법이 불필요하게 된다. 따라서 SAG법은 불포화대에서의 지하수 침투과정을 모사할 때 습윤전선의 이동과 관련하여 발생하는 수치해석적 난제를 크게 개선할 수 있는 방법이다. SAG법과 고정격자를 이용하는 기존의 수정 Picard법을 비교하기 위하여 1차원 침투문제에 대한 수치실험을 실시하였다. 41개의 격자점을 이용한 SAG법은 201점의 고정격자법과 비교하였을 때, 해의 정확도에서는 비슷한 값을 보였으며 계산시간은 반으로 줄어들었다. SAG 해의 질량평형과 수렴도는 시간간격 ($\Delta t$)과 해적응 격자생성에 사용된 가중모수 ($\gamma$)에 크게 영향을 받는 것으로 나타났다. 따라서 SAG법을 이용하여 질량보존적이며 동시에 수렴하는 해를 구하기 위해서는 $\Delta t$와 $\gamma$를 자동으로 재조정하는 과정이 요구되며, 이러한 과정은 계산시간을 증가시키는 요인으로 작용할 수도 있을 것이다. 본 연구에서 제시된 방법은 특별히 시간에 따른 전선의 이동을 다루는 불포화 유동 및 오염물 거동 문제에서 유용하게 사용될 수 있을 것으로 기대된다.

## Introduction

Simulation of groundwater flow in unsaturated porous media is of importance, since the contaminant problems of soil and groundwater are critically influenced by fluid movement in the unsaturated zone. Unsaturated flow in porous media is mostly modeled using Richards' equation (RE) with associated constitutive relations. The formulation of RE is based on the mass conservation principle with the Darcy's law, and the constitutive relations describe the relationship among pressure heads, effective saturations, and relative hydraulic conductivities.

Highly nonlinear property of the constitutive relations makes analytical solutions impossible except for special cases (Barry *et al.*, 1993; Tracy, 1995). Thus, RE is usually solved using various numerical methods such as the finite difference and the finite element methods. During the last two decades, many scientists have involved in simulation of RE and developed numerical models for unsaturated flow in porous media. In general, most of these models tried to solve a system of nonlinear partial differential equations (PDEs) for three forms of RE, using a fixed grid scheme (Milly, 1985; Hills *et al.*,

Department of Geoenvironmental Sciences, Kongju National University, Kongju, Chungnam 314-701, Korea(공주대학교 지질환경과학과)

1989; Celia *et al.*, 1990; Paniconi and Putti, 1994; Rathfelder and Abriola, 1994; Miller *et al.*, 1998). Recently, Kirkland *et al.* (1992) and Pan and Wierenga (1995) introduced transformation methods which can improve solution efficiency compared to standard solution techniques.

One of difficulties encountered in numerical methods for obtaining accurate solutions to RE is that the wetting front, having a high solution-gradient by definition, moves with time. The problem of the resolution near the wetting front is important from the physical point of view as well as the truncation error point of view, since nonlinear process associated with the constitutive relations mainly occurs near the sharp wetting front. In order to handle this problem effectively, it is needed to put more grid points near the sharp wetting front and to put less grid points away from it. Thus, numerical methods using a fixed grid scheme have inherent limitations to obtain accurate solutions to RE. Therefore, it is desirable to employ numerical methods with a moving grid scheme which simultaneously preserves both the computational efficiency and the solution accuracy.

Driven by the needs for a dense grid near the wetting front, some numerical methods have been developed (Lang *et al.*, 1990; Gottardi and Venutelli, 1992; Huang *et al.*, 1994). In general, these adaptive methods can be divided into two categories. One is a moving grid point method in which grid points, without changing the number of points, are moved so that they are concentrated near the wetting front. The r-version method of Lang *et al.* (1990), the moving finite element (MFE) method of Gottardi and Venutelli (1992), and the Eulerian-Lagrangian approach of Huang *et al.* (1994) fall on this category. The other is to add extra grid points near the wetting front. The h-version method of Lang *et al.* (1990) falls on the second category of the adaptive methods.

This paper present a nicely formulated and systematic solution approach to RE which employs a solution-adaptive grid (SAG) method. The method automatically redistributes a fixed number of grid points using a grid generation technique, so that more grid points are concentrated in regions of high solution gradients. The method uses the coordinate transformation technique to employ a new transformed RE, which is solved with the standard finite difference method. Thus, numerical difficulties arising from the movement of the wetting front during the infiltration process can be substantially overcome by the new method. Numerical results for an one-dimensional infiltration problem are presented to compare the SAG method to the modified Picard method (Celia *et al.*, 1990) using a fixed grid.

## Modified Picard Method in a Fixed Grid Scheme

### Richards' equation (RE)

The unsaturated flow in porous media is commonly described by the Richards' equation. RE can be expressed by the following three forms depending on selection of the dependent variable:

$$C(h)\frac{\partial h}{\partial t} = \nabla \cdot K(h)\nabla h + \frac{\partial K}{\partial z} \tag{1}$$

$$\frac{\partial \theta}{\partial t} = \nabla \cdot D(\theta)\nabla \theta + \frac{\partial K}{\partial z} \tag{2}$$

$$\frac{\partial \theta}{\partial t} = \nabla \cdot K(h)\nabla h + \frac{\partial K}{\partial z} \tag{3}$$

where h and $\theta$ are the pressure head and the volumetric water content, respectively; $C = d\theta/dh$ and $D = K/C$ are the specific moisture capacity and the unsaturated diffusivity, respectively; K is the unsaturated hydraulic conductivity; and z is the cartesian coordinate in vertical direction. RE is a nonlinear PDE, since C, D and K vary strongly with h and $\theta$ in unsaturated soils. Thus, in order to solve these equations, associated constitutive relations such as $\theta(h)$ and $K(h)$ are required.

Numerical solutions to the h-based form of (1) have been reported to produce significant mass balance errors and time step limitations (Celia *et al.*, 1990). $\theta$-based form of (2), while it produces reliable mass balance accuracy (Hills *et al.*, 1989), can not be used for layered media with discontinuous $\theta$ profiles and saturated flow conditions. Recently, the mixed form of (3) has been widely used in finite difference or finite element methods, since it produces a perfect mass balance in the solution and simultaneously preserves advantages of the h-based form (Celia *et al.*, 1990; Miller *et al.*, 1998). The numerical method for solving the mixed form of RE will be briefly explained below. A more detailed explanation can be found in Celia *et al.* (1990).

### Modified Picard Algorithm

Applying a backward Euler approximation coupled with a Picard iteration scheme to one-dimensional form of (3) yields

$$\frac{\theta^{n+1,m+1} - \theta^{n}}{\Delta t} = \frac{\partial}{\partial z}\left(K^{n+1,m}\frac{\partial h^{n+1,m+1}}{\partial z}\right) + \frac{\partial K^{n+1,m}}{\partial z} \tag{4}$$

where $n$ and $m$ represent time and iteration level, respectively. A truncated Taylor series expansion of $\theta^{n+1,m+1}$ with respect to h about the point $h^{n+1,m}$ can be expressed as

$$\theta^{n+1,m+1} = \theta^{n+1,m} + \left(\frac{d\theta}{dh}\right)^{n+1,m}(h^{n+1,m+1} - h^{n+1,m}) + O(\delta^2) \tag{5}$$

Assuming $\delta^m \approx h^{n+1,m+1} - h^{n+1,m}$ and substituting (5) into (4) yield a modified Picard approximation;

$$\left(\frac{C^{n+1,m}}{\Delta t}\right)\delta^m - \frac{\partial}{\partial z}\left(K^{n+1,m}\frac{\partial \delta^m}{\partial z}\right)$$

$$= \frac{\partial}{\partial z}\left(K^{n+1,m}\frac{\partial h^{n+1,m}}{\partial z}\right) + \frac{\partial K^{n+1,m}}{\partial z} - \frac{\theta^{n+1,m}-\theta^{n}}{\Delta t} \quad (6)$$

Applying the standard finite difference approximation to z-derivative terms leads to

$$\left(\frac{1}{\Delta t}C_i^{n+1,m}\right)\delta_i^m - \frac{1}{(\Delta z)^2}[K_{i+1/2}^{n+1,m}(\delta_{i+1}^m-\delta_i^m) - K_{i-1/2}^{n+1,m}(\delta_i^m-\delta_{i-1}^m)]$$
$$= +\frac{1}{(\Delta z)^2}[K_{i+1/2}^{n+1,m}(h_{i+1}^{n+1,m}-h_i^{n+1,m}) - K_{i-1/2}^{n+1,m}(h_i^{n+1,m}-h_{i-1}^{n+1,m})]$$
$$+\frac{K_{i+1/2}^{n+1,m}-K_{i-1/2}^{n+1,m}}{\Delta t} - \frac{\theta_i^{n+1,m}-\theta_i^{n}}{\Delta t} \equiv (R_i^{n+1,m})_{MPFD} \quad (7)$$

where the dependent variable is the increment in iteration ($\delta^m$). The right side of (7) is an error measure for the finite difference approximation coupled with the Picard iteration procedure. Thus, convergence of the solution at each time step can be achieved by repeating the Picard iteration procedure until both $\delta^m$ and $R^{n+1,m}$ approach a convergence tolerance.

The internodal hydraulic conductivity $K_{i\pm1/2}$ is evaluated by using the arithmetic average of $K_{i\pm1}$ and $K_i$. Although not a problem of concern in this study, it should be noted that selection of a internodal conductivity scheme can greatly affect the convergence and accuracy of the solution to RE (Desbarats, 1995).

## Constitutive relations

In order to solve RE, constitutive relations, which describe the relationship among pressure heads, effective saturations, and relative hydraulic conductivities, are required. The van Genuchten-Mualem (VGM) relations are most widely used in the literature. The van Genuchten (1980) relation describes the relationship between pressure heads (h) and effective saturations ($S_e$), and the Mualem (1976) relation does between effective saturations ($S_e$) and hydraulic conductivities (K). The equations are written as

$$S_e(h) = \frac{\theta(h)-\theta_r}{\theta_s-\theta_r} = (1+|ah|^n)^{-m} \quad (h \le 0) \quad (8)$$

$$K(S_e) = K_s\sqrt{S_e}[1-(1-S_e^{1/m})^m]^2 \quad (9)$$

where $m = 1 - 1/n$; n and $\alpha$ are fitting parameters related to the uniformity of the pore-size distribution and the mean pore size, respectively; $\theta_s$ and $\theta_r$ are the saturated volumetric water content and the residual volumetric water content, respectively; and $K_s$ is the water-saturated hydraulic conductivity. Based on these closed form VGM relations, the nonlinear parameters ($\theta$ and K) in RE can be calculated.

The specific moisture content (C) in (7) is defined as $C(h) = d\theta/dh$; thus, it can be obtained from the derivative of (8) with respect to h. The resulting equation is

$$C(h) = \frac{(\theta_s-\theta_r)(n-1)|h|^{n-1}\alpha^n}{(1+|\alpha h|^n)^{m+1}} \quad (10)$$

## Solution-Adaptive Grid Method

The basic philosophy of the SAG method is to put more grid points in high gradient regions at a given time. The method is computationally efficient for propagation types of problems, such as movement of the sharp wetting front in unsaturated flow. In the SAG method, the discretization in a problem domain is not stationary, but time-dependent. Thus, the method requires a grid system that is dependent upon the solution gradients at each time step, which should be numerically and automatically generated along with the solution.

The key idea of the method is to simplify the numerical analysis by transforming the physical domain with moving grids to the computational domain with a stationary grid, although the governing equation in the new domain is rather complicated compared to the original one. As will be shown below, if the time derivative term is transformed from the physical domain to the computational domain, no interpolation is required for the movement of grids. Thus, standard finite difference methods can be readily used in the transformed domain without considerations of moving grids in the physical domain.

This adaptive grid technique has been developed and is used extensively in aerodynamics and heat flow areas of study (Eiseman, 1987; Hawken *et al.*, 1991). Recently it also has been applied for groundwater modeling problems with moving boundaries (Koo and Leap; 1998). In the present study, a solution-adaptive grid method based on the finite difference method was developed to solve RE in one-dimensional flow problems. Major emphases were given to the development of a solution method to the transformed RE associated with the modified Picard scheme and a numerical procedure for generating a solution-adaptive grid, particularly in response to movement of the wetting front.

## Coordinate Transformation of RE

The formulation of the SAG method begins with transformation of the governing equation from the physical space to the computational space. Partial derivatives with respect to coordinates in the physical domain (z, t) can be transformed to those in the computational domain ($\xi$, $\tau$) using the chain rule differentiation;

$$\frac{\partial}{\partial z} = \frac{1}{J}\frac{\partial}{\partial \xi} \quad (11)$$

$$\frac{\partial}{\partial t} = \frac{\partial}{\partial \tau} - \frac{1}{J}\frac{\partial z}{\partial \tau}\frac{\partial}{\partial \xi} = \frac{\partial}{\partial \tau} + v\frac{\partial}{\partial \xi} \quad (12)$$

where J is the Jacobian determinant of the inverse transformation given by

$$J = \frac{\partial z}{\partial \xi} \quad (13)$$

Substituting (11) and (12) into (3) leads to the transformed equation of the mixed form RE;

$$\frac{\partial\theta}{\partial\tau} + v\frac{\partial\theta}{\partial\xi} = \frac{1}{J}\frac{\partial}{\partial\xi}\left(\frac{K}{J}\frac{\partial h}{\partial\xi}\right) + \frac{1}{J}\frac{\partial K}{\partial\xi} \tag{14}$$

The second term in the left-hand side of (14) is a pseudo-advective component related to the grid movement in the physical domain. Thus, the movement of grid points is incorporated into the transformed RE, and therefore all computation can be performed on fixed grid points of the transformed domain without using any interpolation techniques. The transformed equation describes the Lagrangian frame of reference, in which the attention is focused not on a fixed point, but on the grid point moving in the physical domain.

## Modified Picard Algorithm for the transformed RE

Again, the modified Picard approximation is applied to the transformed RE. The resulting equation is given by

$$\left(\frac{C^{n+1,m}}{\Delta\tau}\right)\delta^m + v^{n+1}\frac{\partial}{\partial\xi}(C^{n+1,m}\delta^m) - \frac{1}{J^{n+1}}\frac{\partial}{\partial\xi}\left(\frac{K^{n+1,m}}{J^{n+1}}\frac{\partial\delta^m}{\partial\xi}\right)$$
$$= \frac{1}{J^{n+1}}\frac{\partial}{\partial\xi}\left(\frac{K^{n+1,m}}{J^{n+1}}\frac{\partial h^{n+1,m}}{\partial\xi}\right) + \frac{1}{J^{n+1}}\frac{\partial K^{n+1,m}}{\partial\xi}$$
$$-\left(\frac{\theta^{n+1,m}-\theta^n}{\Delta\tau}\right) - v^{n+1}\frac{\partial\theta^{n+1,m}}{\partial\xi} \tag{15}$$

Applying the standard finite difference approximation to $\xi$-derivative terms leads to a discretized formula similar to (7) except the additional pseudo-advective term;

$$\left(\frac{1}{\Delta\tau}C_i^{n+1,m}\right)\delta_i^m + v_i^{n+1}\frac{\partial}{\partial\xi}(C^{n+1,m}\delta^m)$$
$$-\frac{1}{J_i^{n+1}}\left[\frac{K_{i+1/2}^{n+1,m}}{J_{i+1/2}^{n+1}}(\delta_{i+1}^m-\delta_i^m) + \frac{K_{i-1/2}^{n+1,m}}{J_{i-1/2}^{n+1}}(\delta_i^m-\delta_{i-1}^m)\right]$$
$$= \frac{1}{J_i^{n+1}}\left[\frac{K_{i+1/2}^{n+1,m}}{J_{i+1/2}^{n+1}}(h_{i+1}^{n+1,m}-h_i^{n+1,m}) + \frac{K_{i+1/2}^{n+1,m}}{J_{i-1/2}^{n+1}}(h_i^{n+1,m}-h_{i-1}^{n+1,m})\right]$$
$$+\frac{1}{J_i^{n+1}}(K_{i+1/2}^{n+1,m}-K_{i+1/2}^{n+1,m}) - \left(\frac{\theta_i^{n+1,m}-\theta_i^m}{\Delta\tau}\right) - v_i^{n+1}\frac{\partial\theta_i^{n+1,m}}{\partial\xi}$$
$$\equiv (R_i^{n+1,m})_{MPAGFD} \tag{16}$$

where unit grid spacing is used for $\xi$; that is, $\Delta\xi = 1$. The pseudo-velocity term $v_i^{n+1}$ is evaluated by

$$v_i^{n+1} = -\frac{1}{J_i^{n+1}}\left(\frac{z^{n+1}-z^n}{\Delta\tau}\right) \tag{17}$$

For discretization of the advective term, the centered and the upwinding differences are widely used. The centered difference scheme leads to an accurate solution, while it can adversely affect the diagonal dominance of the coefficient matrix. On the other hand, the upwinding difference scheme yields a diagonally dominant matrix, while it introduces an implicit numerical diffusion. Thus, if the advection is relatively small, the centered difference can be suitably used to obtain an accurate solution. For the other case, however, the upwinding scheme is preferred due to its numerical stability. For the upwinding scheme, the advection term is approximated depending on the direction of grid movement, and thus expressed as

$$\frac{\partial}{\partial\xi}(C^{n+1,m}\delta^m) = C_{i+1}^{n+1,m}\delta_{i+1}^m - C_i^{n+1,m}\delta_i^m \quad (v_i^{n+1} \le 0)$$
$$\frac{\partial}{\partial\xi}(C^{n+1,m}\delta^m) = C_i^{n+1,m}\delta_i^m - C_{i-1}^{n+1,m}\delta_{i-1}^m \quad (v_i^{n+1} > 0) \tag{18}$$

Comparative analyses of two schemes used for the SAG method will be presented.

## Numerical Grid Generation

Numerical grid generation is a process of determining the grid in the physical domain which corresponds to the uniform grid in the computational domain. Generation of a solution-adaptive grid is an integral part of the SAG method. A number of grid generation algorithms have been developed. Thompson *et al.* (1985) gives a comprehensive review on numerical grid generation methods.

Among various grid generation methods, partial differential equation (PDE) methods are popular in the literature. PDE methods generate a grid by solving a system of PDEs, of which the most widely used are elliptic equations. According to Knupp and Steinberg (1993), elliptic PDE methods are grouped into two categories: the length generator and the smoothness generator. The length generator takes the physical coordinates to be the solutions of elliptic equations in the transformed domain, while the smoothness generator takes the transformed coordinates to be the solutions in the physical space.

In this study, a length generator with a Laplace-like equation is used for grid generation;

$$\frac{\partial}{\partial\xi}\left(\beta(z)\frac{\partial z}{\partial\xi}\right) = 0 \tag{19}$$

Using an appropriate function for the coefficient ($\beta$), distribution of grid points can be controlled in the physical domain. An exponential control function is used for the coefficient;

$$\beta(z) = e^{-\gamma\left(\frac{z-z_0}{L}\right)^2} \qquad (|z-z_0| \le R)$$
$$\beta(z) = e^{-\gamma\left(\frac{R}{L}\right)^2} \qquad (|z-z_0| > R) \tag{20}$$

where $\gamma$ is the weighting parameter, L is the length of the physical domain, $z_0$ is the location of the wetting front, and R is the radius of weight. $z_0$ can be determined by numerically searching for a grid point which has a maximum gradient of

the solution at each time step. A major limitation of this control function from the numerical point of view is that an appropriate value for $\gamma$ and R should be determined by a heuristic method depending on problems.

Solution-adaptive grids are generated by solving (19) with the associated control function of (20). Dirichlet boundary conditions, $z(1) = 0$ and $z(N) = L$, are applied, so that the grid points are fixed at the boundaries.

### Solution Procedure

For the new time step (n+1), the sequence of algorithm of the SAG method for solving the transformed RE is as follows.

(1) Assuming $z^{n+1} = z^n$, equation (16) is solved to get a temporary solution $h^{n+1}$ using the modified Picard iteration method.

(2) Based on the temporary solution $h^{n+1}$, equation (19) is solved to generate a solution-adaptive grid $z^{n+1}$.

(3) The transformation parameter $J^{n+1}$ is updated.

(4) With new values of $z^{n+1}$ and $J^{n+1}$, equation (16) is solved again to get a new solution $h^{n+1}$.

During the modified Picard iteration, the Thomas algorithm is applied for solving a system of linear equations that has a tridiagonal coefficient matrix, and iteration is repeated until a convergence is achieved for both $\delta^m$ and $R^{n+1,m}$. In order to increase the solution accuracy, multiple grid generation could be executed for each time step by repeating the sequence (2), (3), and (4). However, a test showed that a desirable distribution of grid points was achieved by two iterations, and further iterations did not change the solution.

## Numerical Results

A series of numerical experiments for simulating infiltration of the wetting front into an initially dry soil were performed to test robustness of the SAG method.

### Fixed Grid Method of Celia *et al.* (1990)

For the purpose of comparative analyses of the SAG method to the standard fixed grid method, numerical solutions of Celia *et al.* (1990) were reproduced by solving (7) with the VGM relations. The values of the parameters used in the VGM equations are: $n = 2$, $\alpha = 0.0335$ cm$^{-1}$, $\theta_s = 0.368$, $\theta_r = 0.102$, and $K_s = 0.00922$ cm/s. $h(z, 0) = -1000$ cm is used for the initial condition, and $h(0, t) = -1000$ cm and $h(100 \text{ cm}, t) = -75$ cm are used for the boundary conditions.

Solution profiles at 24 hours of transient simulations are presented in Figures 1 and 2, for different time steps and for different grid spacings, respectively. Figure 1 shows that the solutions of the modified Picard iteration method are insensitive to $\Delta t$. As shown in Figure 2, however, the wetting front is more diffused, and infiltration depths of the wetting front are overestimated as $\Delta z$ increases. Thus, as Celia *et al.* (1990) mentioned, the solutions of the modified Picard iteration method are greatly influenced by the spacial truncation errors.

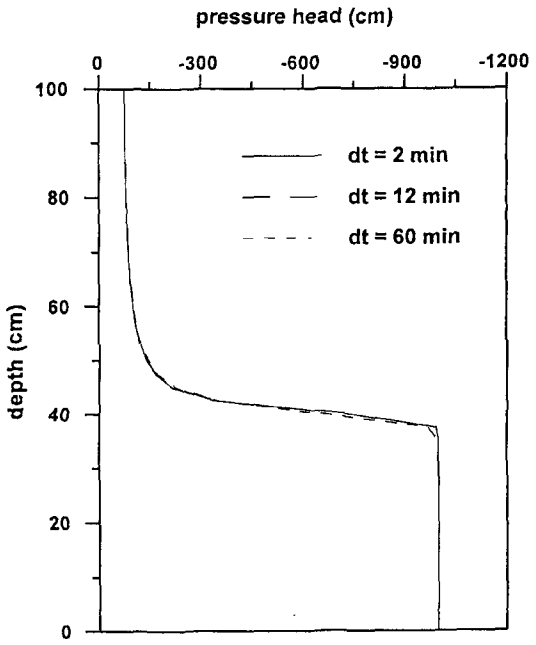


**Figure 1.** Simulated solution profiles using the fixed grid method for different time steps.

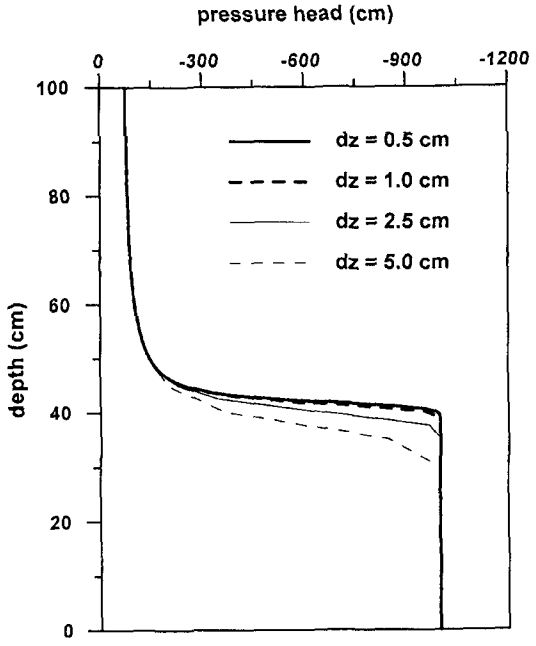


**Figure 2.** Simulated solution profiles using the fixed grid method for different grid spacings.

### SAG Method

For the same infiltration problem, several numerical solu-

tions were obtained using the SAG method. Figure 3 shows numerical solutions using both the fixed grid method and the SAG method with $\Delta t = 1$ hour. The dashed line and the bold solid line indicate solutions using the fixed grid method with $\Delta z = 2.5$ cm and 0.5 cm; thus, the number of grid points (N) is 41 and 201, respectively. The solid lines with symbols indicate solutions of the SAG method for different values of the weighting parameter ($\gamma$) in Eqn. (20). All of them used the same number of grid points ($N = 41$) and the same radius of weight ($R = 25$). Figure 3 presents that, if an appropriate value of the weighting parameter is used, the SAG method with $N = 41$ could produce the solution with the same accuracy as that of the fixed grid method with $N = 201$. It is shown, on the contrary, that the infiltration depth of the wetting front could be underestimated if the value of the weighting parameter is too high.

The distributions of moving grid points for $\gamma = 2$, 6, 10, and 14 are shown in Figures 4a, 4b, 4c, and 4d, respectively. They clearly show that the grid points are progressively redistributed in accordance with downward movement of the wetting front, resulting in a dense grid near the wetting front.

Computational efficiency was evaluated on the basis of CPU time. In Table 1, the CPU times for six simulations are presented. All the simulations were performed using an IBM PC with 64 Mbytes of RAM and 200 MHz of the processor speed. The CPU time for the SAG method is significantly enhanced as $\gamma$ increases. This is mainly due to the fact that

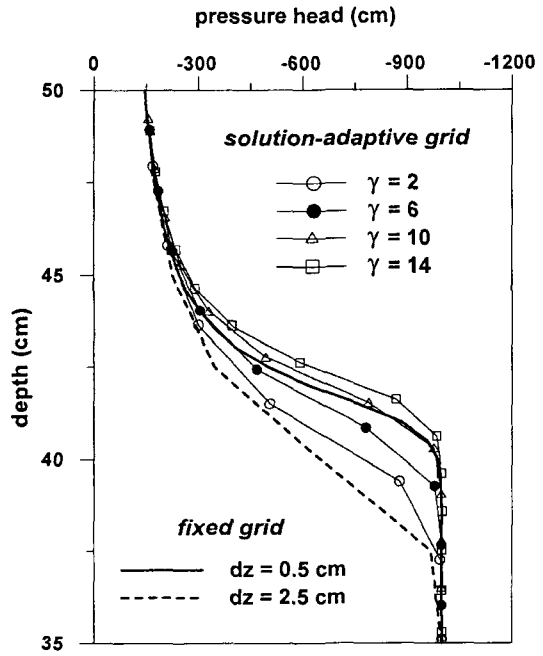


**Figure 3.** Comparison of solution profiles using the fixed grid method and the SAG method.

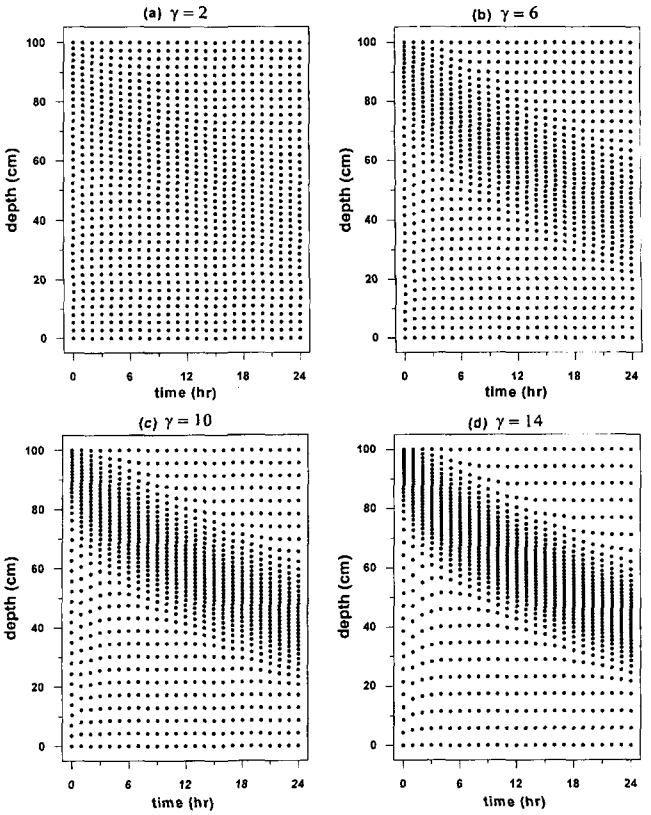


**Figure 4.** Distributions of moving grid points for different weighting parameters: (a) $\gamma = 2$, (b) $\gamma = 6$, (c) $\gamma = 10$, and (d) $\gamma = 14$.

**Table 1.** Comparison of the computing time of six simulations performed in the present study

| method | N | $\gamma$ | R (cm) | CPU time (sec) |
|---|---|---|---|---|
| fixed grid | 41 | – | – | 1.05 |
| | 201 | – | – | 9.28 |
| adaptive grid | 41 | 2 | 25 | 2.91 |
| | 41 | 6 | 25 | 3.74 |
| | 41 | 10 | 25 | 4.61 |
| | 41 | 14 | 25 | 6.04 |

the convergence of the Picard iteration scheme exhibited strong dependence on the magnitude of the pseudo-advection term of (14); that is, more Picard iterations are required for a simulation that uses higher value of $\gamma$, resulting in increase of the CPU time. The SAG method seems to produce some improvements in computational costs, if considered that the method using $\gamma = 10$ yields a solution with the same accuracy as the fixed grid method with $N = 201$, while it requires only half of the CPU time. This result demonstrates one of the most attractive feature of the SAG method; that is, the ability to obtain solutions with much less computational effort and grid points than required by the fixed grid method, with no loss of accuracy.

Figures 5 and 6 present solution profiles obtained when the

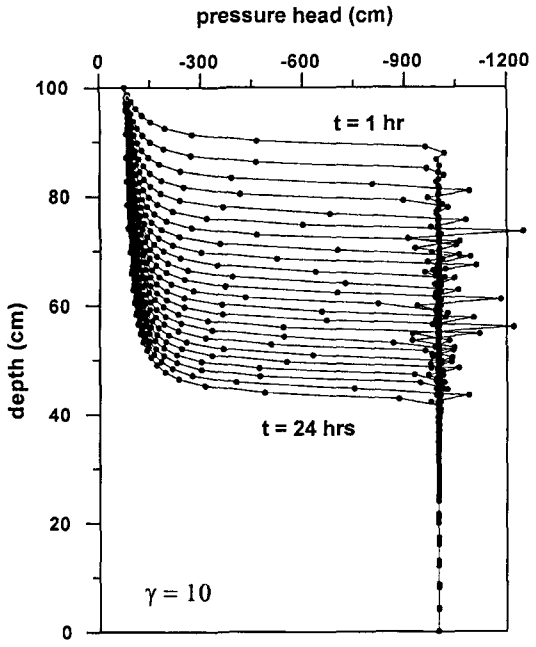


**Figure 5.** Solution profiles using the centered difference scheme for the pseudo-advection term.

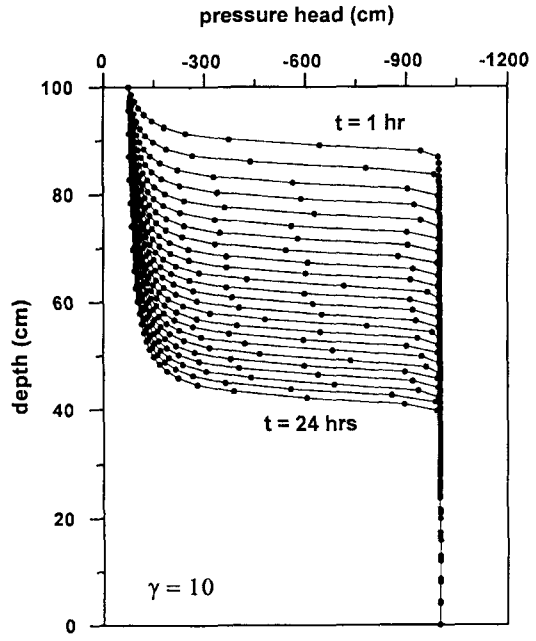


**Figure 6.** Solution profiles using the upwinding difference scheme for the pseudo-advection term.

centered difference and the upwinding difference schemes are applied to the pseudo-advection term, respectively. In Figure 5, the numerical solution of the centered difference scheme exhibits a spacial oscillation over several nodal points ahead of the wetting front, which is an unrealistic physical process. This oscillatory behavior of the solution can be explained by rewriting (16) as follows:

$$\left(-\frac{1}{2}a_{i-1}-d_{i-1}\right)\delta_{i-1}^{m}+(1+d_{i-1}+d_{i+1})\delta_{i}^{m}$$
$$+\left(\frac{1}{2}a_{i+1}-d_{i+1}\right)\delta_{i+1}^{m}=\frac{\Delta\tau}{C_i}(R_i^{n+1,m}) \tag{21}$$

where $a_{i\pm1}$ and $d_{i\pm1}$ are the advection number and the diffusion number, respectively. They are written as

$$a_{i\pm1}=\frac{v_i C_{i\pm1}\Delta\tau}{\Delta\xi C_i} \tag{22}$$

$$d_{i\pm1}=\frac{K_{i\pm1/2}\Delta\tau}{\Delta\xi J_{i\pm1/2}J_i C_i} \tag{23}$$

From (22) and (23), the Peclet number of the SAG method can be defined as

$$P_{i\pm1}=\frac{a_{i\pm1}}{d_{i\pm1}}=\frac{v_i C_{i\pm1}J_i J_{i\pm1/2}\Delta\xi}{K_{i\pm1/2}} \tag{24}$$

Substituting (24) into (21) yields

$$d_{i-1}\left(-\frac{1}{2}P_{i-1}-1\right)\delta_{i-1}^{m}+(1+d_{i-1}+d_{i+1})\delta_{i}^{m}$$
$$+d_{i+1}\left(\frac{1}{2}P_{i+1}-1\right)\delta_{i+1}^{m}=\frac{\Delta\tau}{C_i}(R_i^{n+1,m}) \tag{25}$$

The coefficient of $\delta_i^m$ and the diffusion number $d_{i\pm1}$ are always positive. Thus, if the coefficient of either $\delta_{i-1}^m$ or $\delta_{i+1}^m$ becomes positive, the contribution of $\delta_{i\pm1}^m$ to $\delta_i^m$ is negative, which is physically incorrect and causes oscillatory behavior in the solution. Consequently, the following grid velocity criterion should be satisfied to obtain physically correct solutions with no oscillation;

$$-2\frac{K_{i-1/2}}{C_{i-1}J_i J_{i-1/2}\Delta\xi}\le v_i\le 2\frac{K_{i+1/2}}{C_{i+1}J_i J_{i+1/2}\Delta\xi} \tag{26}$$

Figure 7 shows grid points that do not satisfy (26); that is, $P_{i-1}<-2$ or $P_{i+1}>2$. Most of these points are located in the region ahead of the wetting front, which is in dry conditions. As shown in Figure 8, the ratio of the specific moisture content to the unsaturated hydraulic conductivity increases as the pressure head decreases, or as the soil becomes drier. Therefore, the degree of oscillations would be affected by the initial condition of soils as well as the grid velocity.

On the other hand, the upwinding scheme gives

$$d_{i-1}\left(-\frac{1}{2}[P_{i-1},0]-1\right)\delta_{i-1}^{m}+(1+d_{i-1}+d_{i+1}+[P_{i-1}-P_{i+1}])\delta_{i}^{m}$$
$$d_{i+1}\left(-\frac{1}{2}[-P_{i+1},0]-1\right)\delta_{i+1}^{m}=\frac{\Delta\tau}{C_i}(R_i^{n+1,m}) \tag{27}$$

where the bracket [A, B] denotes the maximum value between A and B. The upwinding coefficients of $\delta_{i\pm1}^m$ are always negative, and this guarantees no oscillation in the solution. Thus, the oscillation was eliminated in the upwinding difference scheme as shown in Figure 6. For this reason, the upwinding scheme is preferred for the present study.

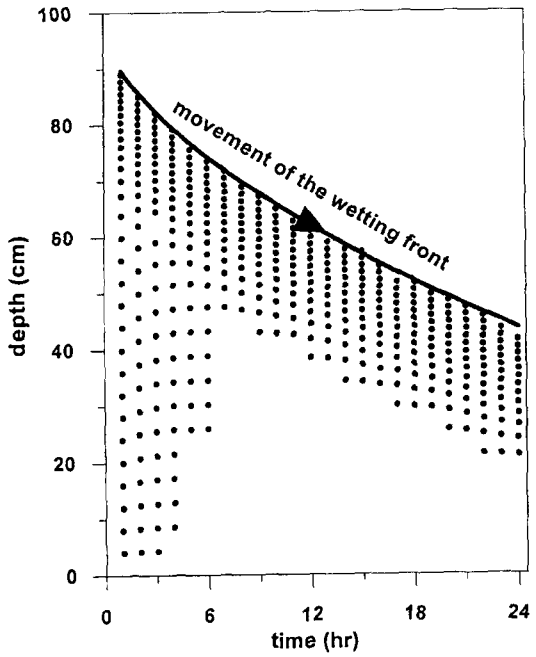


**Figure 7.** Grid points that do not satisfy Equation (26).

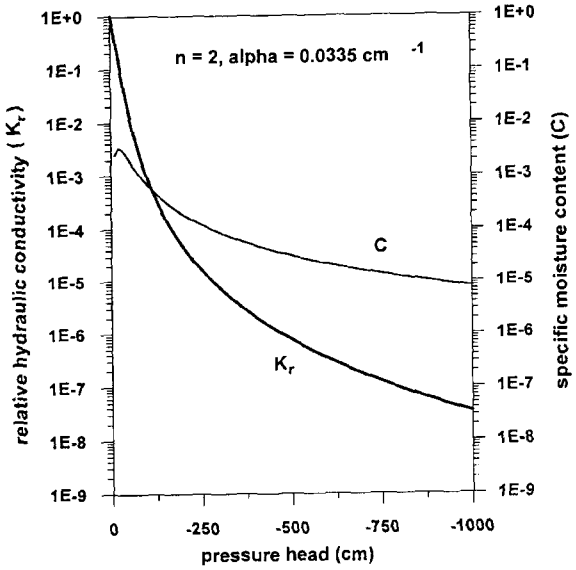


**Figure 8.** Soil characteristics by the VGM relations.

## Mass Balance Errors of the SAG method

The global mass balance was calculated for all the simulations to measure the capability of the SAG method in mass conservation. The mass balance is defined as a ratio of the total mass added into the domain to the total net flux into the domain; thus, it can be expressed as

$$MB_{SAG} = \frac{\frac{1}{2}\sum_{i=1}^{N-1}[(\theta_i^n + \theta_{i+1}^n)(z_{i+1}^n - z_i^n) - (\theta_i^0 + \theta_{i+1}^0)(z_{i+1}^0 - z_i^0)]}{\sum_{j=1}^{n}\left[K_{N-1/2}^j\left(\frac{h_N^j - h_{N-1}^j}{z_N^j - z_{N-1}^j} + 1\right) - K_{1-1/2}^j\left(\frac{h_2^j - h_1^j}{z_2^j - z_1^j} + 1\right)\right]\cdot \Delta t^j} \quad (28)$$

As shown in Figure 9, the fixed grid method employing the modified Picard iteration scheme produces a perfect mass balance regardless of time step sizes (Celia *et al.*, 1990). Unfortunately, however, the SAG method produces a moderate decline of the mass balance as either $\Delta t$ or $\gamma$ increases. Because $\Delta t$ and $\gamma$ are certainly related to the pseudo-advection, the mass balance error is likely attributed to the truncation errors in upwinding differencing of the pseudo-advection term. The modified differential equation (MDE) for the transformed RE could provide information on the truncation errors associated with the upwinding difference scheme. A detailed explanation on the MDE can be found in Hoffman (1992).

Therefore, contrary to the fixed grid method, the SAG method requires time step limitations in maintaining mass balance; that is, the computer code could be modified to automatically adjust the time step size according to the calculated mass balance. Thus, mass balance errors can be greatly reduced in the SAG method by employing an automated readjustment of the time step size, which is not considered in this study.

## Convergence of the SAG method

With varying the time step size, convergence behavior of the Picard iteration scheme for the SAG method was examined for the same infiltration problem. The number of Picard iterations are generally increased for higher value of $\Delta t$, and oscillations of the solution occurred from one iteration to the next at all time steps after a breakpoint of $\Delta t$, which resulted

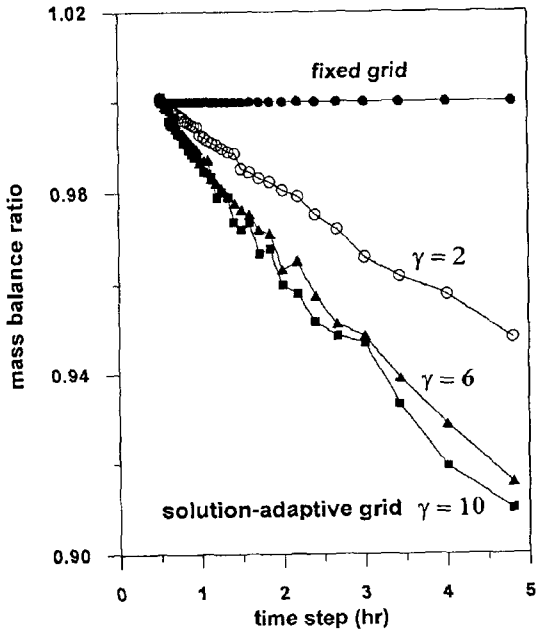


**Figure 9.** Mass balance error versus time step size for different weighting parameters.

in no convergence of the solution. The under-relaxation method is used to enhance convergence of the Picard iteration scheme when oscillations are encountered during the iteration. The method updates solutions using both values at the current and previous iteration levels; that is,

$$h^{n+1,m+1} = \Omega h^{n+1,m+1} + (1-\Omega)h^{n+1,m} \quad (29)$$

where $\Omega$ represents the relaxation parameter. In this study, $\Omega$ is initially set to $\Omega = 1$ (no relaxation), and reduced by a factor of 0.1 whenever the number of Picard iterations exceeds the maximum number of iterations specified in the code for termination. Thus, the code is designed to successively reduce $\Omega$ when convergence of the solution is very slow, or oscillation occurs. Figure 10 presents variations of the relaxation parameter versus $\Delta t$. Figure 10 indicates that the increase of either $\Delta t$ or $\gamma$ adversely affects convergence of the solution. Similar to the mass balance, the convergence is strongly related to the relative magnitude of the pseudo-advection term. Thus, the SAG method can be further improved by incorporating an automated procedure of readjusting $\Delta t$ and $\gamma$ which virtually yields a mass-conservative and convergent solution.

### Extension of the method to multi-dimensions

In terms of conceptual formulation, the SAG method introduced in this study for solving one-dimensional RE can be readily extended to multi-dimensions. However, transformation in multi-dimensions will give cross-derivative terms in the transformed RE, which are quite troublesome when applying the finite difference method. Thus, a somewhat different discretization scheme should be used to handle cross-derivatives. For solving a system of linear equations, iterative methods rather than the Thomas algorithm should be employed. Multi-dimensional version of (19) may be used for generating solution-adaptive grids. However, the control function should be formulated in a different way, since the location of the wetting front is not a point, but a line or a surface in multi-dimensions. The SAG method is being extended to two-dimensional unsaturated flow problems by the author.

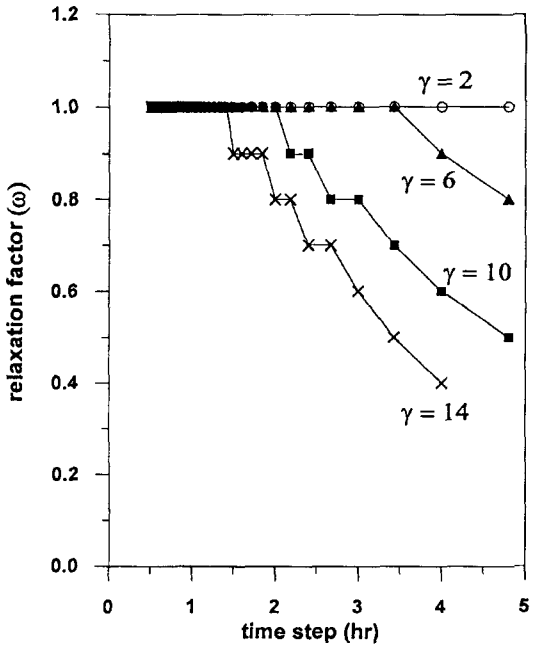


**Figure 10.** Relaxation parameter ($\Omega$) versus time step size for different weighting parameters.

## Conclusions

The SAG method was introduced as an effective numerical technique for solving unsaturated flow problems. Based on comparative analyses of the SAG method and traditional fixed grid method for an infiltration problem, the following conclusions are drawn:

1. The proposed equation for the generation of an adaptive grid consistently produced a dense grid near the wetting front through the simulation. The only limitation of the equation is that an appropriate value of the weighting parameter should be determined by trial and error calculations.

2. The use of an adaptive grid did not increase the computer time, even though more computations are necessary. This is due to improved convergence properties of the solution as well as use of fewer grid points (Anderson and Rai, 1982).

3. For two discretization schemes of the pseudo-advection term examined, the upwinding scheme is superior to the centered difference, since the latter scheme exhibited oscillatory behavior of the solution ahead of the wetting front.

4. Although the traditional method achieved a perfect mass balance for all time step sizes, the SAG method demonstrated that it progressively becomes more deteriorated as either the time step size or the weighing parameter increases. Therefore, although not considered in this study, the mass balance can be used to dynamically adjust the time step size or the weighting parameter.

5. The SAG method is an attractive alternative to the traditional fixed grid method for solving unsaturated flow and other transport problems involving the propagation of a sharp-front.

## Acknowledgment

This research was supported by the Research Institute of Natural Science at Kongju National University.

## References


Anderson, D. A. and Rai, M. M., 1982, The use of solution adaptive grids in solving partial differential equations, Numerical Grid Generation, edited by Joe F. Thompson, North-Holland.

Barry, D. A., Parlanga, J. Y., Sander, G. G. and Sivlaplan, M., 1993, A class of exact solutions for Richards' equation, J. Hydrol., 142, 29-46.

Celia, M. A., Bouloutas, E. T. and Zarba, R. L., 1990, A general mass-conservative numerical solution for the unsaturated flow equation, Water Resour. Res., 26, 1483-1496.

Celia, M. A., Ahuja, L. R. and Pinder, G. F., 1987, Orthogonal collocation and alternating-direction procedures for unsaturated flow problems, Adv. Water Resour., 10, 178-187.

Desbarats, A. J., 1995, An interblock conductivity scheme for finite difference models of steady unsaturated flow in heterogeneous media, Water Resour. Res., 31, 2883-2889.

Eiseman P. R., 1987, Adaptive grid generation, Comput. Meth. Appl. Mech. Eng., 64, 321-376.

Gottardi, G. and Venutelli, M., 1992, Moving finite element model for one-dimensional infiltration in unsaturated soil, Water Resour. Res., 28, 3259-3267.

Hawken D. F., Gottlieb, J. J. and Hansen, J. S., 1991, Review of some adaptive node-movement techniques in finite-element and finite-difference solutions of partial differential equations, J. Comp. Phys., 95, 254-302.

Huang, K., Zhang, R. and van Genuchten, M. T., 1994, An Eulerian-Lagrangian approach with an adaptively corrected method of characteristics to simulate variably saturated water flow, Water Resour. Res., 30, 499-507.

Hills, R. G., Porro, I., Hudson, D. B. and Wierenga, P. J., 1989, Modeling one-dimensional infiltration into very dry soils, 1. Model development and evaluation, Water Resour. Res., 25, 1259-1269.

Hoffman, J. D., 1992, Numerical methods for engineers and Scientists, McGraw-Hill, pp 825.

Kirkland, M. R., Hills, R. G. and Wierenga, P. J., 1992, Algorithms for solving Richards' equation for variably saturated soils, Water Resour. Res., 28, 2049-2058.

Knupp, P. and Steinberg, S., 1993, Fundamentals of Grid Generation, CRC Press, pp 263.

Koo, M. H. and Leap, D. I., 1998, Modeling three-dimensional groundwater flows by the body-fitted coordinate (BFC) method: II. Free and moving boundary problems, Transport in Porous Media, 30, 345-362.

Lang J. R., Abriola, L. M. and Gamliel, A., 1990, Comparison of P, H, and R-version adaptive finite element solutions for unsaturated flow in porous media, Proceedings of the Eighth International Conference on Computational Methods in Water Resources, Venice, Italy, 187-192, Springer-Verlag, New York.

Miller C. T., Williams, G. A., Kelly, C. T. and Tocci, M. D., 1998, Robust solution of Richards' equation for nonuniform porous media, Water Resour. Res., 34, 2599-2610.

Milly, P. C. D., 1985, A mass-conservative procedure for time-stepping in models of unsaturated flow, Adv. Water Resour., 8, 32-36.

Mualem, Y., 1976, A new model for predicting the hydraulic conductivity of unsaturated porous media, Water Resour. Res., 12, 513-522.

Pan, L. and Wierenga, P. J., 1995, A transformed pressure head-based approach to solve Richards' equation for variably saturated soils, Water Resour. Res., 31, 925-931.

Paniconi, C. and Putti, M., 1994, A comparison of Picard and Newton iteration in the numerical solution of multidimensional variably saturated flow problems, Water Resour. Res., 30, 3357-3374.

Rathfelder, K. and Abriola, L. M., 1994, Mass conservative numerical solutions of the head-based Richards equation, Water Resour. Res., 30, 2579-2586.

Thompson, J. F., Warsi, Z. U. A. and Mastin, C. W., 1985, Numerical grid generation: Fundamentals and applications, North-Holland, Elsevier, New York, pp 483.

Tracy, F. T., 1995, 1-D, 2-D, and 3-D analytical solutions of unsaturated flow in groundwater, J. Hydrol., 170, 199-214.

van Genuchten, M. T., 1980, A closed-form equation for predicting the hydraulic conductivity of unsaturated soils, Soil Sci. Soc. Am. J., 44, 892-898.